TRACKING PERFORMANCE OF AN ADAPTIVE TRANS-MIT BEAMSPACE BEAMFORMER IN DYNAMIC MISO WIRELESS CHANNELS

S. S. I. Hussain, J. Bigham, and C. Parini [†]

Electronic Engineering Department
Queen Mary, University of London (QMUL)
Mile End Road, London E1 4NS, UK

M. I. Shiekh

Electrical Engineering Department
University of Engineering & Technology (UET)
GT Road, Lahore, Pakistan

Abstract—This paper presents the performance of an Adaptive Transmit Beamspace Beamformer (ATBBF) in a dynamic channel for Multiple Input Single Output (MISO) per user wireless system. An ATBBF consists of several transmit beamformers on the Transmit Antenna Array (TAA). The antenna weights of each Transmit Beamformer (TB) are held constant while its input is weighted by an adaptive beamspace weight. A Beamspace Gradient Sign Feedback (BGSF) algorithm updates these beamspace weights. The performance metric of an ATBBF is derived and analyzed in a dynamic channel undergoing Rayleigh fading independently at the antennas. A performance comparison between an ATBBF and a TB having adaptive antenna weights is made in terms of convergence and tracking of various slow and fast fading channels by simulations. Both Full Dimension (FD) and Reduced Dimension (RD) ATBBFs are considered. Comparisons show that the FD ATBBF gives a performance equivalent to that of a TB and outperforms the RD ATBBF. Thus the FD ATBBF can provide beamforming gain and fading diversity similar to that of a TB. Furthermore, the performance of the FD ATBBF improves on increasing the number of antenna elements of the TAA.

[†] S. S. I. Hussain is also with Electrical Engineering Department, University of Engineering & Technology (UET), GT Road, Lahore, Pakistan.

1. INTRODUCTION

The evolution of Third Generation (3G) Wideband Code Division Multiple Access (WCDMA) to Beyond Third Generation (B3G) Long Term Evolution (LTE) wireless communication system has resulted in specifying that wireless and multimedia services are asymmetrical in terms of data requirement, with downlink having higher traffic than uplink [1]. Moreover, current base stations have dual receive antenna diversity to improve uplink performance in terms of single user link and system capacity [2]. To have the same receive diversity at the Mobile Station (MS) in downlink is a costly addition for users of small portable voice terminals. Their small physical sizes necessitates multiple antennas to be closely spaced. This often increases correlation among received signals that leads to reduced diversity gain [2]. This correlation also restricts capacity enhancements offered by Multiple Input Multiple Output (MIMO) systems [3]. Thus a practical and cost effective increase in downlink capacity can be achieved by having multiple antennas only at the base station, i.e., having a Multiple Input Single Output (MISO) system [4].

Both WCDMA and LTE support Frequency Division Duplex (FDD) [5, 6]. In FDD, downlink and uplink channels in a multipath environment are generally not the same, and the measured uplink channel cannot be directly applied as a reciprocal downlink. For the MISO FDD system, spatial diversity and beamforming become the two main downlink multiantenna schemes [5, 6]. Spatial diversity provides maximum performance gain when the channels from the base station antennas to the mobile are uncorrelated. Large antenna spacing on the order of several carrier wavelengths for the Transmit Antenna Array (TAA) at the base station leads to uncorrelated channels [4]. Techniques based on Space Time Codes (STC) provide diversity [7] and coding gain for multiple receive antennas. For a single receive antenna, STC provides diversity gain only. This gain will reduce if fading channels across multiple antennas become correlated [8].

Downlink Beamforming is achieved by a Transmit Beamformer (TB). A TB combines a TAA with a signal processor to adapt antenna weights of the array. These weights determine the array factor of a TAA [9]. The baseband waveform of a user is replicated into multiple streams equivalent to the number of antenna elements in the array. Each stream is multiplied by an antenna specific adaptive complex base band weight. It is then fed to its antenna through the transceiver for subsequent transmission [9]. This allows the TB, to transmit coded bits in a way that they are received coherently at the mobile station. Furthermore, this forms a beam with maximum gain in the

direction of the desired mobile [2]. Antenna spacings for a TB are required to be typically half the wave length to prevent spatial domain aliasing [2, 10]. Secondly, the TB has to launch a beam into the propagation environment, so that each user gets its signal without interference from signals intended for other users [11]. In contrast, a Receive Beamformer (RB) aims to spatially filter the single user signal by formation of a beam or beams in the signal processor [9, 12]. Hence transmit and receive beamforming are substantially different in nature [13], with the former affecting all receivers, while the latter can be implemented independently at each receiver without disturbing other links [14].

A TB requires knowledge of the downlink channel to set its adaptive weights. Methods based on utilizing the measured uplink channel characteristics (e.g., angle of arrival and angular dispersion) to infer the downlink characteristics require correlation between receive antennas. These methods do not provide fading diversity, as in the case of independent fading at the antennas there is no correlation between receive antennas [8]. To provide both fading diversity and beamforming gain in FDD systems, feedback of the channel coefficients from the mobile to the TB is required. Various algorithms have been proposed to decrease this feedback [8, 15–17]. Their tracking performance in slow and fast fading channels with independent fading at the antennas reveals that they outperform STC in slow fading channels and are outperformed by STC in fast fading channels [8, 15]. Beamforming techniques in B3G LTE and Fourth Generation (4G) LTE-Advanced systems are variants of the above techniques tailored for MIMO [6, 18].

In [19], an innovative approach based on an Adaptive Transmit Beamspace Beamformer (ATBBF) was proposed for downlink beamforming. In an ATBBF multiple streams of a user signal are equal to the number of transmit beamformers with each stream assigned to a TB. A stream is multiplied by its respective adaptive complex base band beamspace weight and then fed to its TB. The outputs of each TB for an antenna are summed at the base band level before being fed to that antenna through the transceiver [9]. The beam pattern of each TB is steered towards a different direction. Updating a beamspace weight results in altering only the magnitude of this beam pattern, while its steered direction remains constant. The Gradient Sign Feedback (GSF) algorithm [8] was modified so that instead of updating antenna weights of the TB, beamspace weights of the ATBBF were updated [19]. Comparisons between this ATBBF and a TB with GSF algorithm for a static channel showed an approximately similar performance [19]. This paper compares their performance for dynamic channels. In Section 2, the system model consisting of an ATBBF in a

dynamic channel is described. Details of the Beamspace Gradient Sign
Feedback (BGSF) algorithm for a dynamic channel are in Section 3.
In Section 4, the performance of an ATBBF in a dynamic channel
undergoing Rayleigh fading is derived. Performance comparisons can
be found in Section 5, which is followed by the conclusion.

2. SYSTEM MODEL

The system model consists of an ATBBF at the base station of
a MISO per user WCDMA wireless system in a dynamic channel.
WCDMA utilizes the Direct Sequence Code Division Multiple Access
(DS-CDMA) and FDD methods. Performance metric of an ATBBF in
this system is also derived.

2.1. ATBBF

A TAA is a Uniform Linear Array (ULA) having N isotropic antenna
elements with half wave length inter element spacing. Furthermore,
TAA is aligned along the z-axis at the base station. The ATBBF
consists of M transmit beamformers on the TAA.

In a Full Dimension Adaptive Transmit Beamspace Beamformer
(FD ATBBF) $M = N$, while in a Reduced Dimension Adaptive
Transmit Beamspace Beamformer (RD ATBBF) $M < N$. Each of the
M transmit beamformers has a constant weight vector of size $N \times 1$ for
the antenna elements of the TAA. Among the M transmit beamformers
there is always one TB that weighs each antenna element of the TAA
uniformly, i.e., its beam pattern is directed towards broadside. In a FD
ATBBF, weight vectors for other transmit beamformers are chosen so
that their beam patterns are directed on either side of broadside and
are uniformly spread out in the total spatial span of a ULA. This gives
a total of $M = N$ transmit beamformers/beam patterns of the FD
ATBBF [10]. These beam patterns are ideally mutually orthogonal;
hence, they are called orthogonal beams [10]. For a RD ATBBF a
reduced set of $M < N$ orthogonal beams are selected from among the
$M = N$ orthogonal beams of the FD ATBBF.

The matrix consisting of $N \times M$ antenna weights of all transmit
beamformers is called the beamspace matrix $\mathbf{B}_{bs}$, where the mth
column of $\mathbf{B}_{bs}$ represents the weight vector of the mth TB. The
weight vector of each TB is normalized by N so that the maximum
beamforming gain provided by a TB in its steered direction is $0\,\text{dB}$.
These weight vectors and hence columns of $\mathbf{B}_{bs}$ are also mutually
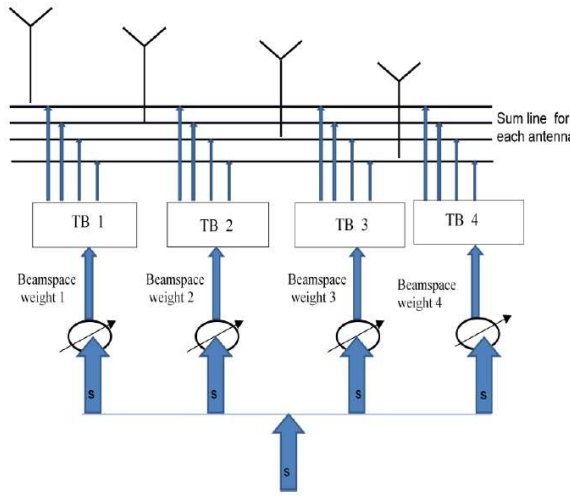orthogonal [10].

Figure 1. Schematic diagram of a $M = N = 4$ FD ATBBF.

$$\mathbf{B}_{bs}^{H}\mathbf{B}_{bs} = \frac{\mathbf{I}}{N} \qquad (1)$$

The signal to be transmitted s is replicated M times and each replica is fed to an adaptive beamspace weight of a TB as shown in Figure 1. The $M \times 1$ beamspace weight vector $\mathbf{w}_{bs}$, consists of beamspace weights of all M transmit beamformers. The $M \times 1$ vector $\mathbf{x}_{bs}$, is the output when input signal s is processed by $\mathbf{w}_{bs}$.

$$\mathbf{x}_{bs} = \mathbf{w}_{bs}s \qquad (2)$$

Each single element of $\mathbf{x}_{bs}$ is processed by a weight vector of a respective TB to get a $N \times 1$ output vector. These M output vectors are added to get a resultant $N \times 1$ transmit signal vector $\mathbf{t}$ for the TAA. In matrix notation these two steps are accomodated in the following matrix multiplication:

$$\mathbf{t}=\mathbf{B}_{bs}\mathbf{x}_{bs}=\mathbf{B}_{bs}\mathbf{w}_{bs}s \qquad (3)$$

2.2. Transmit Signal

The Nyquist sampling theorem has been applied to the system model for appropriate discrete time signal representation. If n is the Nyquist sampling time index, $s_{traffic}(n)$ is the transmitted sequence and $P_{traffic}^{(T)}$

is the transmit power, then the signal vector tranmitted by the ATBBF from (3) becomes:

$$\mathbf{t}\left(n\right) = \sqrt{P_{traffic}^{(T)}} \; \frac{\mathbf{B}_{bs}\mathbf{w}_{bs}(i)}{\|\mathbf{B}_{bs}\mathbf{w}_{bs}(i)\|} s_{traffic}(n) \tag{4}$$

Here i is the time index denoting the ith iteration number of the BGSF algorithm. Therefore $\mathbf{w}_{bs}(i)$ is the beamspace weight vector of the ATBBF in the ith iteration of the BGSF. The product $\mathbf{B}_{bs}\mathbf{w}_{bs}(i)$ has been normalized by its norm, so that the direction of the product is taken into account rather than its magnitude. The simplification of this norm from the Hermitian transpose property [10] and (1) is:

$$\|\mathbf{B}_{bs}\mathbf{w}_{bs}(i)\| = \sqrt{(\mathbf{B}_{bs}\mathbf{w}_{bs}(i))^H \mathbf{B}_{bs}\mathbf{w}_{bs}(i)} = \sqrt{\mathbf{w}_{bs}^H(i)\mathbf{B}_{bs}^H\mathbf{B}_{bs}\mathbf{w}_{bs}(i)}$$

$$= \sqrt{\frac{\mathbf{w}_{bs}^H(i)\mathbf{w}_{bs}(i)}{N}} = \frac{\|\mathbf{w}_{bs}(i)\|}{\sqrt{N}} \tag{5}$$

Hence $\mathbf{t}\left(n\right)$ becomes

$$\mathbf{t}\left(n\right) = \sqrt{P_{traffic}^{(T)}} \; \frac{\mathbf{B}_{bs}\mathbf{w}_{bs}(i)\sqrt{N}}{\|\mathbf{w}_{bs}(i)\|} s_{traffic}(n) \tag{6}$$

2.3. Dynamic Channel

The dynamic channel in this model is a flat fading channel, i.e., it consists of a single time resolvable path. Thus there is only a single channel coefficient associated with each antenna element of the TAA. The $N \times 1$ channel vector $\mathbf{c}$ consists of all these N channel coefficients. A complex fading channel coefficient is usually modeled as a correlated complex Gaussian random process with Rayleigh distributed amplitudes and phases [20, 21]. This is achieved here by modelling each coefficient of $\mathbf{c}$ as a first order Autoregressive (AR1) [10] complex Gaussian process with a zero mean complex Gaussian stimulus $\mathbf{x}$ [8, 15].

$$\mathbf{c}\left(i+1\right) = a\mathbf{c}\left(i\right) + \mathbf{x}(i) \tag{7}$$

Here i is the time index denoting the ith update interval of the channel. This i is the same as in (4) indicating that the channel and the beamspace weights are being updated at the same rate. The parameter a indicates the fading rate of the channel. To verify that an ATBBF can provide fading diversity, the channel is taken to be uncorrelated across the antennas, i.e.,

$$E\left(\mathbf{x}(i)\mathbf{x}^H(i)\right) = 2\sigma^2 \mathbf{I} \tag{8}$$

Uncorrelated fading is possible for half wave length antenna spacing and appropriate angle spread as can be inferred from [22].

2.4. Received Signal

Assuming no pilot signal, the received signal at the mobile with perfect channel estimation for demodulation becomes

$$r\left(n\right) = \sqrt{P_{traffic}^{(T)}}\ \mathbf{c}^{H}(i)\frac{\mathbf{B}_{bs}\mathbf{w}_{bs}(i)\sqrt{N}}{\|\mathbf{w}_{bs}(i)\|}s_{traffic}\left(n\right) + z(n) \qquad (9)$$

where $z(n)$ is the received complex zero mean Gaussian noise with variance $2\sigma^2$.

2.5. Performance Metric of ATBBF

The total usable signal power $P^{(R)}$ at the mobile is the square of received signal voltage divided by the unit resistance [23]. The first term on the right side of (9) is the received signal voltage, hence $P^{(R)}$ becomes

$$P^{(R)} = \left[\sqrt{P_{traffic}^{(T)}}\ \mathbf{c}^{H}(i)\frac{\mathbf{B}_{bs}\mathbf{w}_{bs}(i)\sqrt{N}}{\|\mathbf{w}_{bs}(i)\|}s_{traffic}\left(n\right)\right]$$

$$\left[\sqrt{P_{traffic}^{(T)}}\ \mathbf{c}^{H}(i)\frac{\mathbf{B}_{bs}\mathbf{w}_{bs}(i)\sqrt{N}}{\|\mathbf{w}_{bs}(i)\|}s_{traffic}\left(n\right)\right]^{H}$$

The power of the modulated signal sequence $|s_{traffic}(n)|^2$ is assumed one. From the Hermitian transpose property the above equation becomes

$$= \frac{NP_{traffic}^{(T)}}{\mathbf{w}_{bs}(i)^{2}}\left[\ \mathbf{c}^{H}(i)\mathbf{B}_{bs}\mathbf{w}_{bs}(i)\right]\left[\mathbf{w}_{bs}^{H}(i)\mathbf{B}_{bs}^{H}\mathbf{c}(i)\right] \qquad (10)$$

Each of the terms in the two brackets is a scalar quantity. Scalar multiplication is commutative, reversing the sequence of the two terms does not affect the product. Defining the $N \times N$ channel correlation matrix $\mathbf{R}(i)$ [4] as:

$$\mathbf{R}(i) = \mathbf{c}(i)\mathbf{c}^{H}(i) \qquad (11)$$

Inserting $\mathbf{R}(i)$ in (10)

$$= \frac{NP_{traffic}^{(T)}}{\|\mathbf{w}_{bs}(i)\|^{2}}\mathbf{w}_{bs}^{H}(i)\mathbf{B}_{bs}^{H}\mathbf{R}(i)\mathbf{B}_{bs}\mathbf{w}_{bs}(i)$$

The performance metric J is the ratio of the received and transmit powers that becomes:

$$J(i) = \frac{P^{(R)}}{P^{(T)}_{traffic}} = \frac{N\mathbf{w}_{bs}^H(i)\mathbf{B}_{bs}^H\mathbf{R}(i)\mathbf{B}_{bs}\mathbf{w}_{bs}(i)}{\|\mathbf{w}_{bs}(i)\|^2}$$

$$= \frac{(\mathbf{B}_{bs}\mathbf{w}_{bs}(i))^H\mathbf{R}(i)\mathbf{B}_{bs}\mathbf{w}_{bs}(i)}{\|\mathbf{B}_{bs}\mathbf{w}_{bs}(i)\|^2} \tag{12}$$

3. ALGORITHM DESCRIPTION

The BGSF algorithm is concerned with the selection of beamspace weights of an ATBBF that can maximize the ATBBF's performance in a dynamic channel. The BGSF updates the ATBBF's beamspace weights at the base station of a WCDMA system as given below.

3.1. At the Base Station Transmitter

The traffic signal transmitted by the ATBBF with beamspace weights $\mathbf{w}_{bs}(i)$ in the ith update interval is given in (6). For the pilot signal defined in the WCDMA system, two beamspace weight vectors $\mathbf{w}_{bs_{even}}(i)$ and $\mathbf{w}_{bs_{odd}}(i)$ are derived from $\mathbf{w}_{bs}(i)$ as follows:

$$\mathbf{w}_{bs_{even}}(i) = \mathbf{w}_{bs}(i) + \|\mathbf{w}_{bs}(i)\|\beta\mathbf{p}(i) \tag{13}$$

$$\mathbf{w}_{bs_{odd}}(i) = \mathbf{w}_{bs}(i) - \|\mathbf{w}_{bs}(i)\|\beta\mathbf{p}(i) \tag{14}$$

Here β is the adaption rate parameter and $\mathbf{p}$ is the $M \times 1$ test perturbation vector. The test perturbation vector is generated as a complex, zero mean, normal Gaussian vector with an auto correlation matrix of $2\mathbf{I}$. It is clear from Equations (13) and (14) that $\mathbf{w}_{bs}$ is the mean of $\mathbf{w}_{bs_{even}}$ and $\mathbf{w}_{bs_{odd}}$. A time slot of duration K is defined as an integral multiple of the Nyquist sampling index (n). The pilot signal is sent with $\mathbf{w}_{bs_{even}}$ during even slots $\left(\lfloor\frac{n}{K}\rfloor = even\right)$ and with $\mathbf{w}_{bs_{odd}}$ in odd slots $\left(\lfloor\frac{n}{K}\rfloor = odd\right)$. The update interval i is an integral multiple of $2K$ times the Nyquist sampling time interval. All weights are held constant during the ith measurement interval. Total transmit signal during this interval becomes:

$$t(n) = \sqrt{P^{(T)}_{traffic}} \frac{\mathbf{B}_{bs}\mathbf{w}_{bs}(i)\sqrt{N}}{\|\mathbf{w}_{bs}(i)\|} s_{traffic}(n)$$

$$+ \sqrt{P^{(T)}_{pilot}}\mathbf{B}_{bs}s_{pilot}(n)\sqrt{N} \left\{ \begin{matrix} \frac{\mathbf{w}_{bs_{even}}(i)}{\|\mathbf{w}_{bs_{even}}(i)\|} & if\left(\lfloor\frac{n}{K}\rfloor = even\right) \\ \frac{\mathbf{w}_{bs_{odd}}(i)}{\|\mathbf{w}_{bs_{odd}}(i)\|} & if\left(\lfloor\frac{n}{K}\rfloor = odd\right) \end{matrix} \right\} \tag{15}$$

Here $s_{pilot}(n)$ is the pilot sequence modulation and $P^{(T)}_{pilot}$ is the mean pilot channel transmission power.

3.2. At the Mobile Receiver

The received signal is the channel passed data and pilot signal, to which noise is added, i.e.,

$$r(n) = \sqrt{P^{(T)}_{traffic}} \frac{\mathbf{c}^H(i)\mathbf{B}_{bs}\mathbf{w}_{bs}(i)\sqrt{N}}{\|\mathbf{w}_{bs}(i)\|} s_{traffic}(n)$$

$$+\sqrt{P^{(T)}_{pilot}}\mathbf{c}^H(i)\mathbf{B}_{bs}s_{pilot}(n)\sqrt{N}\left\{ \begin{array}{l} \frac{\mathbf{w}_{bs_{even}}(i)}{\|\mathbf{w}_{bs_{even}}(i)\|} \ if\ \left(\lfloor\frac{n}{K}\rfloor=even\right) \\ \frac{\mathbf{w}_{bs_{odd}}(i)}{\|\mathbf{w}_{bs_{odd}}(i)\|} \ if\ \left(\lfloor\frac{n}{K}\rfloor=odd\right) \end{array} \right\}+z(n) \quad (16)$$

Code multiplexing can make $s_{pilot}(n)$ and $s_{traffic}(n)$ orthogonal to each other and hence they can be separated at the receiver. Power delivered by the pilot signal for even and odd slots from (12) becomes as follows:

$$P^{(R)}_{pilot_{even}} = \frac{NP^{(T)}_{pilot}}{\|\mathbf{w}_{bs_{even}}(i)\|^2}\mathbf{w}^H_{bs_{even}}(i)\mathbf{B}^H_{bs}\mathbf{R}(i)\mathbf{B}_{bs}\mathbf{w}_{bs_{even}}(i) \quad (17)$$

$$P^{(R)}_{pilot_{odd}} = \frac{NP^{(T)}_{pilot}}{\|\mathbf{w}_{bs_{odd}}(i)\|^2}\mathbf{w}^H_{bs_{odd}}(i)\mathbf{B}^H_{bs}\mathbf{R}(i)\mathbf{B}_{bs}\mathbf{w}_{bs_{odd}}(i) \quad (18)$$

It must be noted that the two products $\mathbf{B}_{bs}\mathbf{w}_{bs_{even}}(i)$ and $\mathbf{B}_{bs}\mathbf{w}_{bs_{odd}}(i)$ have been normalized in (15). Therefore, the power delivered to the receiver by the pilot weights in (17) and (18) is dependent upon their direction rather than their magnitudes. The mobile receiver will sum $P^{(R)}_{pilot_{even}}$ and $P^{(R)}_{pilot_{odd}}$ for all the respective even and odd slots in the ith interval and then compare them as follows:

$$d(i) = \int P^{(R)}_{pilot_{even}} - \int P^{(R)}_{pilot_{odd}} \quad (19)$$

Feedback to the base station becomes as follows

$$feedback(i) = sign(d(i)) \quad (20)$$

The comparison generates a $+1$ feedback if received power in the even slot is greater than the received power in the odd slot, while it is -1 for vice versa.

3.3. Returning to the Base Station Transmitter

The above feedback updates $\mathbf{w}_{bs}$ at the transmitter as follows:

if $(feedback\,(i) == +1)$

$$\mathbf{w}_{bs}\,(i+1) = \mathbf{w}_{bs_{even}}(i) \qquad (21)$$

elseif $(feedback\,(i) == -1)$

$$\mathbf{w}_{bs}\,(i+1) = \mathbf{w}_{bs_{odd}}(i) \qquad (22)$$

Feedback indicates which of the two pilot channels delivers more power to the mobile. The beamspace weight vector of the indicated pilot channel is chosen as $\mathbf{w}_{bs}$ for the next update interval $(i+1)$.

4. PERFORMANCE ANALYSIS IN AR1 CHANNEL

The performance metric of the ATBBF given in (12) can be simplified for a AR1 channel having a single resolvable path, because $\mathbf{R}(i)$ becomes a rank one matrix. Eigen analysis of $\mathbf{R}(i)$ will give only one non-zero eigenvalue $\lambda_0(i)$ with its corresponding eigenvector $\mathbf{q}_0(i)$ equivalent to the normalized channel vector, i.e.,

$$\mathbf{q}_0(i) = \frac{\mathbf{c}(i)}{\|\mathbf{c}(i)\|} \qquad (23)$$

All other eigenvalues $\lambda_1(i), \ldots, \lambda_{N-1}(i)$ of $\mathbf{R}(i)$ are zero and their corresponding eigenvectors $\mathbf{q}_1\,(i)\,, \ldots, \mathbf{q}_{N-1}\,(i)$ are arbitrary within the space orthogonal to the channel vector called the null space. Secondly, eigen analysis reveals that any arbitrary vector having the same dimensions as that of an eigenvector can be expressed as a linear combination of eigenvectors [24]. The product $\mathbf{B}_{bs}\mathbf{w}_{bs}\,(i)$ is $N \times 1$ vector and can be expressed as:

$$\mathbf{B}_{bs}\mathbf{w}_{bs}\,(i) = \int_{l=0}^{l=N-1} u_l(i)\,\mathbf{q}_l\,(i) \qquad (24)$$

where the coefficients u_l are called the eigenweights of the product $\mathbf{B}_{bs}\mathbf{w}_{bs}\,(i)$. A specific set of two eigenvectors where the first is $\mathbf{q}_0(i)$, while the second is the normalized projection of $\mathbf{B}_{bs}\mathbf{w}_{bs}\,(i)$ on to the null space can be imposed in (24) because all other eigenvectors $\mathbf{q}_1\,(i)\,, \ldots, \mathbf{q}_{N-1}\,(i)$ are arbitrary within the null space. The first eigenvector represents the desired weight vector while the second eigenvector is the error vector. Thus (24) becomes

$$\mathbf{B}_{bs}\mathbf{w}_{bs}\,(i) = u_0\,(i)\,\mathbf{q}_0\,(i) + u_1\,(i)\,\mathbf{q}_1\,(i) \qquad (25)$$

The projection matrix onto the channel vector $\mathbf{c}(i)$ from [10] is

$$\mathbf{c}(i)\left[\mathbf{c}^H(i)\mathbf{c}(i)\right]^{-1}\mathbf{c}^H(i) = \mathbf{c}(i)\left(\|\mathbf{c}(i)\|^{\mathbf{2}}\right)^{-1}\mathbf{c}^H(i) = \frac{\mathbf{c}(i)\mathbf{c}^H(i)}{\|\mathbf{c}(i)\|^{\mathbf{2}}} \qquad (26)$$

Thus the projection matrix onto the null space becomes

$$\left(\mathbf{I} - \frac{\mathbf{c}\left(i\right)\mathbf{c}^{H}\left(i\right)}{\left\| \mathbf{c}\left(i\right) \right\|^{2}} \right) \tag{27}$$

Hence projection of $\mathbf{B}_{bs}\mathbf{w}_{bs}\left(i\right)$ on to the null space is

$$\left(\mathbf{I} - \frac{\mathbf{c}\left(i\right)\mathbf{c}^{H}\left(i\right)}{\left\| \mathbf{c}\left(i\right) \right\|^{2}} \right) \mathbf{B}_{bs}\mathbf{w}_{bs}\left(i\right) \tag{28}$$

Normalized value of the above projection is the second eigenvector $\mathbf{q}_1\left(i\right)$, i.e.,

$$\mathbf{q}_1\left(i\right) = \frac{\left(\mathbf{I} - \frac{\mathbf{c}(i)\mathbf{c}^{H}(i)}{\|\mathbf{c}(i)\|^{2}} \right) \mathbf{B}_{bs}\mathbf{w}_{bs}\left(i\right)}{\left\| \left(\mathbf{I} - \frac{\mathbf{c}(i)\mathbf{c}^{H}(i)}{\|\mathbf{c}(i)\|^{2}} \right) \mathbf{B}_{bs}\mathbf{w}_{bs}\left(i\right) \right\|} \tag{29}$$

Eigenweights $u_0(i)$ and $u_1(i)$ in (25) are given from [24]:

$$u_0\left(i\right) = \mathbf{q}_0^{H}(i)\,\mathbf{B}_{bs}\mathbf{w}_{bs}\left(i\right) \tag{30}$$

$$u_1\left(i\right) = \mathbf{q}_1^{H}(i)\,\mathbf{B}_{bs}\mathbf{w}_{bs}\left(i\right) \tag{31}$$

Substituting the value of $\mathbf{q}_0\left(i\right), \mathbf{q}_1\left(i\right)$ from (23) and (29) into (30) and (31) respectively

$$u_0\left(i\right) = \frac{\mathbf{c}^{H}\left(i\right)}{\left\| \mathbf{c}\left(i\right) \right\|}\mathbf{B}_{bs}\mathbf{w}_{bs}\left(i\right) \tag{32}$$

$$
\begin{aligned}
u_1 &= \left(\frac{\left(\mathbf{I} - \frac{\mathbf{c}(i)\mathbf{c}^{H}(i)}{\|\mathbf{c}(i)\|^{2}} \right) \mathbf{B}_{bs}\mathbf{w}_{bs}\left(i\right)}{\left\| \left(\mathbf{I} - \frac{\mathbf{c}(i)\mathbf{c}^{H}(i)}{\|\mathbf{c}(i)\|^{2}} \right) \mathbf{B}_{bs}\mathbf{w}_{bs}\left(i\right) \right\|} \right)^{H} \mathbf{B}_{bs}\mathbf{w}_{bs}\left(i\right) \\
&= \frac{\mathbf{w}_{bs}^{H}(i)\mathbf{B}_{bs}^{H}\left(\mathbf{I} - \frac{\mathbf{c}(i)\mathbf{c}^{H}(i)}{\|\mathbf{c}(i)\|^{2}} \right)^{H}}{\left\| \left(\mathbf{I} - \frac{\mathbf{c}(i)\mathbf{c}^{H}(i)}{\|\mathbf{c}(i)\|^{2}} \right) \mathbf{B}_{bs}\mathbf{w}_{bs}\left(i\right) \right\|}\mathbf{B}_{bs}\mathbf{w}_{bs}\left(i\right)
\end{aligned} \tag{33}
$$

For convenience eigenweight energies are defined as the square of the magnitude of corresponding eigenweights, i.e.,

$$v_0\left(i\right) = \left| u_0\left(i\right) \right|^{2} = \left| \frac{\mathbf{c}^{H}\left(i\right)\mathbf{B}_{bs}\mathbf{w}_{bs}\left(i\right)}{\left\| \mathbf{c}\left(i\right) \right\|} \right|^{2} \tag{34}$$

$$v_1\left(i\right) = \left| u_1\left(i\right) \right|^{2} = \left| \frac{\mathbf{w}_{bs}^{H}(i)\mathbf{B}_{bs}^{H}\left(\mathbf{I} - \frac{\mathbf{c}(i)\mathbf{c}^{H}(i)}{\|\mathbf{c}(i)\|^{2}} \right)^{H}\mathbf{B}_{bs}\mathbf{w}_{bs}\left(i\right)}{\left\| \left(\mathbf{I} - \frac{\mathbf{c}(i)\mathbf{c}^{H}(i)}{\|\mathbf{c}(i)\|^{2}} \right) \mathbf{B}_{bs}\mathbf{w}_{bs}\left(i\right) \right\|} \right|^{2} \tag{35}$$

Therefore $v_0(i)$ gives the portion of the energy of $\mathbf{B}_{bs}\mathbf{w}_{bs}(i)$ that is in the direction of the mobile and received by it. $v_1(i)$ represents that portion of energy of $\mathbf{B}_{bs}\mathbf{w}_{bs}(i)$ that is not received by the mobile and is called error energy. The performance metric J of the ATBBF is simplified in terms of eigenweight energies $v_0(i), v_1(i)$ as shown below:

$$J(i) = \frac{(\mathbf{B}_{bs}\mathbf{w}_{bs})^H \mathbf{R}(i)\,\mathbf{B}_{bs}\mathbf{w}_{bs}}{\|\mathbf{B}_{bs}\mathbf{w}_{bs}\|^2}$$

$$= \frac{[u_0(i)\,\mathbf{q}_0(i) + u_1(i)\,\mathbf{q}_1(i)]^H \mathbf{R}(i)\,[u_0(i)\,\mathbf{q}_0(i) + u_1(i)\,\mathbf{q}_1(i)]}{\|u_0(i)\,\mathbf{q}_0(i) + u_1(i)\,\mathbf{q}_1(i)\|^2}$$

$$J(i) = \frac{\left[u_0^H(i)\ u_1^H(i)\right]\begin{bmatrix}\mathbf{q}_0^H(i)\\\mathbf{q}_1^H(i)\end{bmatrix}\left[\mathbf{q}_0(i)\ \mathbf{q}_1(i)\right]\begin{bmatrix}\lambda_0(i)&0\\0&0\end{bmatrix}\begin{bmatrix}\mathbf{q}_0^H(i)\\\mathbf{q}_1^H(i)\end{bmatrix}\left[\mathbf{q}_0(i)\ \mathbf{q}_1(i)\right]\begin{bmatrix}u_0(i)\\u_1(i)\end{bmatrix}}{|u_0(i)|^2 + |u_1(i)|^2}$$

$$J(i) = \frac{\lambda_0(i)\,|u_0(i)|^2}{|u_0(i)|^2 + |u_1(i)|^2} = \frac{v_0(i)\,\lambda_0(i)}{v_0(i) + v_1(i)} \tag{36}$$

λ_0 is equal to the Rayleigh quotient of its corresponding eigenvector $\mathbf{q}_0$ and is given from [24] as

$$\lambda_0(i) = \frac{\mathbf{q}_0^H(i)\,\mathbf{R}(i)\,\mathbf{q}_0(i)}{\|\mathbf{q}_0(i)\|^2} = \frac{\frac{\mathbf{c}^H(i)}{\|\mathbf{c}(i)\|}\mathbf{c}(i)\,\mathbf{c}^H(i)\frac{\mathbf{c}(i)}{\|\mathbf{c}(i)\|}}{\left\|\frac{\mathbf{c}(i)}{\|\mathbf{c}(i)\|}\right\|^2}$$

$$= \frac{\frac{\|\mathbf{c}(i)\|^2\|\mathbf{c}(i)\|^2}{\|\mathbf{c}(i)\|^2}}{\frac{\|\mathbf{c}(i)\|^2}{\|\mathbf{c}(i)\|^2}} = \|\mathbf{c}(i)\|^2 \tag{37}$$

Inserting this value of λ_0 in (36) we get:

$$J(i) = \frac{v_0(i)}{v_0(i) + v_1(i)}\lambda_0(i) = \frac{v_0(i)}{v_0(i) + v_1(i)}\|\mathbf{c}(i)\|^2 \tag{38}$$

Thus for the given channel vector $\mathbf{c}(i)$, the performance metric $J(i)$ of the ATBBF depends upon the ratio of the received energy $v_0(i)$ to the sum of the received and error energies $v_0(i) + v_1(i)$. This ratio is denoted by $J'(i)$, i.e.,

$$J'(i) = \frac{v_0(i)}{v_0(i) + v_1(i)} \tag{39}$$

Therefore if the error energy $v_1(i)$ is zero then $J'(i)$ attains its maximum value of one (or 0 dB). $J(i)$ then becomes equal to $\|\mathbf{c}(i)\|^2$ and the ATBBF delivers maximum power. Performance metric of a TB in AR1 Rayleigh fading is also dependent upon the ratio $J'(i)$ [8].

5. PERFORMANCE SIMULATIONS IN AR1 CHANNEL

The performance simulations generate performance curves of an ATBBF and a TB in an AR1 Rayleigh flat fading channel as described in (7) and (8). The set of values of the fading rate a chosen to represent different fading channels are:

$$a = [0.999, \ 0.9968, \ 0.99, \ 0.968, \ 0.9, \ 0.6, \ 0.3, \ 0] \qquad (40)$$

Small values of a indicate fast fading channels, while its large values represent slow fading channels. For both ATBBF and TB, a performance curve is generated for each value of a. The ordinate axis of a performance curve represents the ratio $J'(i)$ of an ATBBF or TB in dB's. Both the BGSF and GSF algorithm of an ATBBF and TB respectively have an adaption rate parameter β. The abscissa of a performance curve consists of the following set of β values:

$$\beta = [0.0013, \ 0.0022, \ 0.004, \ 0.007, \ 0.013, \ 0.022, \ 0.04, \ 0.07, \ 0.13,$$
$$0.22, \ 0.4, \ 0.7, \ 1.3] \qquad (41)$$

Each curve is obtained by taking the mean value of $J'(i)$ of an ATBBF or a TB for $1,000,000$ iterations of BGSF or GSF respectively. In each ith iteration the beamspace weights or antenna weights of the ATBBF or TB are updated by BGSF or GSF algorithms respectively, along with the update of AR1 channel coefficients. The performance curves become independent of the initial channel coefficients and the variance σ^2 given in (8) for this number of iterations.

The performance curves of a FD ATBBF ($M = N = 2$) are shown in Figure 2, where the curve of the slowest fading channel $a = 0.999$
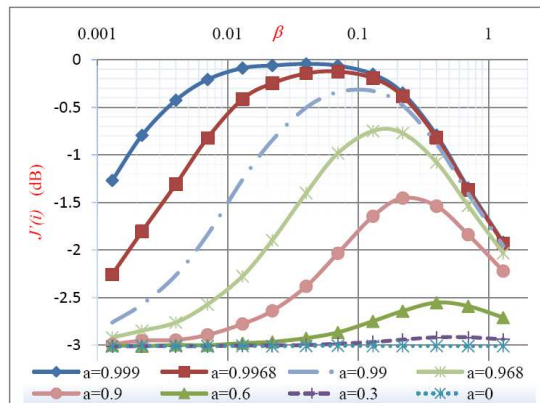

Figure 2. Performance curves of FD ATBBF for $N = 2$.
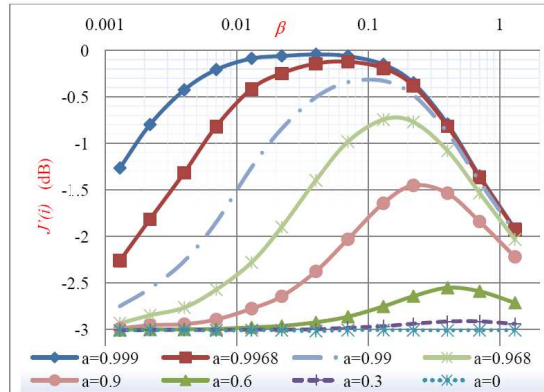
Figure 3. Performance curves of TB for $N = 2$.

has the maximum magnitude. As the fading rate increases, magnitude of the curve decreases, which is why the fastest fading channel $a = 0$ has the lowest magnitude. In slow fading, due to the slowly varying channel, the FD ATBBF has the time to perturb its beamspace weights in the right direction before considerable change in the channel takes place. In fast fading, by the time the FD ATBBF acquires the required beamspace weights, the channel changes considerably. For a performance curve of a particular fading rate the value of β that gives its maximum value is called its β_{max} value. The β_{max} for the curve of the slowest fading channel $a = 0.999$ is minimum. It increases with the increase in the fading rate. This is because the FD ATBBF has to accommodate more change in its beamspace weights in fast fading channels.

The performance curves of the TB for $N = 2$ are shown in Figure 3. On comparing the curves of the FD ATBBF and TB for $N = 2$, it becomes evident that at any fading rate both give the same performance. For $N = 4$ antennas, FD ATBBF and TB curves are shown in Figures 4 and 5 respectively. The variation in the maximum value and the β_{max} value of the performance curve with the increase in fading rate is similar to that described for $N = 2$ antennas. Similarly, the performance of the FD ATBBF and TB for $N = 4$ antennas over all slow and fast fading rates of the channel has the same magnitude as was seen for $N = 2$ antennas.

Performance curves for $N = 2$ are also compared with those for $N = 4$. It is observed that at any fading rate the maximum value of a curve for $N = 2$ is approximately two times its maximum value for $N = 4$ in terms of dB's. The reason is that the number of
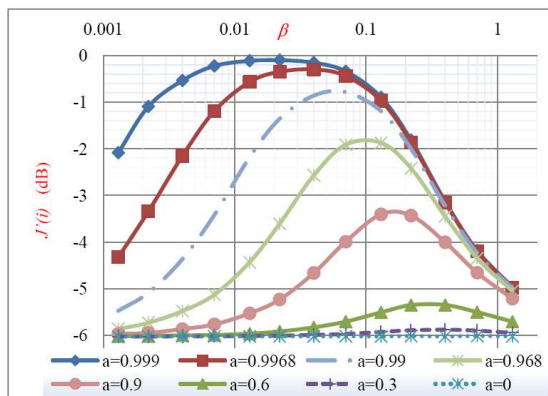
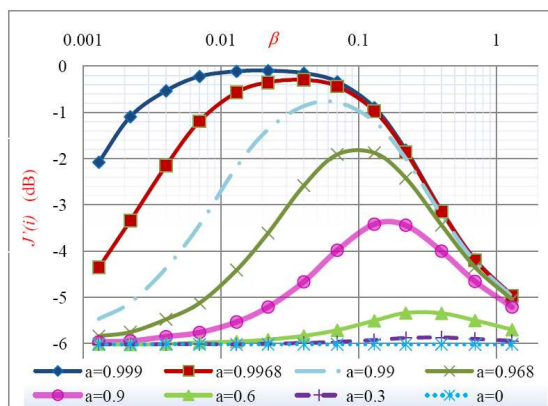**Figure 4.** Performance curves of FD ATBBF for $N = 4$.

Figure 5. Performance curves of TB for $N = 4$.

adaptive weights for $N = 2$ is half than that for $N = 4$ resulting in shorter convergence time of beamspace weights for the former. A greater magnitude of $J'(i)$ for $N = 2$ does not translate into a greater magnitude of $J(i)$. $J(i)$ from (38) depends on the product of $J'(i)$ and square of the channel vector norm $\|\mathbf{c}(i)\|^2$. $\|\mathbf{c}(i)\|^2$ for $N = 2$ and $N = 4$ gives a 3.01 dB and 6.02 dB array gain respectively. On adding array gain to the performance curves of $N = 2$ and $N = 4$, $J(i)$ of the FD ATTBF for $N = 4$ acquires greater magnitude than for $N = 2$ in all fading channels.

Both RD and FD ATBBF have the same value of N and hence equivalent value of $\|\mathbf{c}(i)\|^2$. Thus their performance comparison
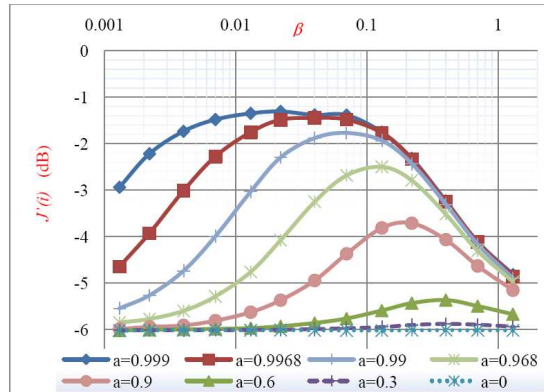
Figure 6. Performance curves of RD ATBBF for $M = 3$; $N = 4$.

depends only on their value of $J'(i)$. Performance curves of RD ATBBF in the above AR1 channels are generated for three cases $M = 1$, $N = 4$; $M = 2$, $N = 4$; & $M = 3$, $N = 4$. Performance of the highest magnitude is obtained for $M = 3$, $N = 4$ RD ATBBF (given in Figure 6). This is due to the fact that among the three cases $M = 3$, $N = 4$ RD ATBBF has the largest number of orthogonal beams in the total spatial span. This same reason causes the RD ATBBF to be outperformed by $M = N = 4$ FD ATBBF for all fading rates, as observed on comparing Figure 6 with Figure 4 respectively. Figure 6 also illustrates that the variation in the maximum value and the $\beta_{\max}$ value of the performance curve with the increase in fading rate is similar to that for the FD ATBBF.

6. CONCLUSIONS

The tracking performance of an ATBBF in a dynamic channel has been presented. An ATBBF consists of M transmit beamformers on a TAA having N antenna elements with $M \leq N$. Each TB has a constant $N \times 1$ weight vector for the TAA. In an ATBBF the signal to be transmitted is fed to the TB through an adaptive beamspace weight, which is updated by BGSF. Performance of the ATBBF is analysed in a flat fading dynamic channel with a single time resolvable path. The channel coefficients are undergoing AR1 Rayleigh fading that is uncorrelated across the N antenna elements. Different fading rates are applied to represent slow and fast fading channels. The performance results are plotted for a FD ATBBF, TB and RD ATBBF.

The results illustrate that the RD and FD ATBBF give maximum

performance in slow fading channels, while performance decreases in fast fading channels. In slow fading both the RD and FD ATBBF are able to track the channel effectively. In fast fading the channel changes at a rate that is greater than the ability of the RD and FD ATBBF to acquire and keep track of the optimal beamspace weights. Secondly, the $\beta_{\max}$ value of a performance curve for both the RD or FD ATBBF increases with the increase in the fading rate. This is because a greater value of β is required to bring more change in the beamspace weights of the RD or FD ATBBF to track fast fading channels.

For the same number of antenna elements, the FD ATBBF and TB give a similar performance in a single time resolvable path AR1 channel. Hence the FD ATBBF can provide the same beamforming gain and fading diversity as by a TB.

On comparing the performance of the FD ATBBF for $N = 2$ and $N = 4$, it is observed that without incorporating the array gain, maximum performance of the former is approximately double than that of the latter in terms of dB's. The reason is that the number of adaptive beamspace weights for $N = 2$ is half than that for $N = 4$ resulting in shorter convergence time of beamspace weights and improved performance for the former. On adding array gain, performance for $N = 4$ acquires greater magnitude than for $N = 2$ in all fading channels.

The RD ATBBF gives its best performance in the above AR1 channels when it has the greatest number of orthogonal beams in the total spatial span. The FD ATBBF outperforms the RD ATBBF because it will always have more orthogonal beams in the total spatial span.

ACKNOWLEDGMENT

REFERENCES

1. Fazel, K. and S. Kaiser, *Multi-carrier and Spread Spectrum Systems*, 2nd edition, John Wiley & Sons Ltd., 2008.
2. Rohani, K., M. Harrison, and K. Kuchi, "A comparison of base station transmit diversity methods for third generation cellular

standards," *Proc. IEEE Vehicular Technology Conference*, Vol. 1, 351–355, May 1999.

3. Chizhik, D., G. J. Foschini, M. J. Gans, and R. A. Valenzuela, "Keyholes, correlations, and capacities of multi-element transmit and receive antennas," *IEEE Transactions On Wireless Communications*, Vol. 1, No. 2, 361–368, April 2002.

4. Derryberry, R. T., S. D. Gray, D. M. Ionescu, G. Mandyam, and B. Raghothaman, "Transmit diversity in 3G CDMA systems," *IEEE Communications Magazine*, 68–75, April 2002.

5. Dakdouki, A. S., V. L. Banket, N. K. Mykhaylov, and A. A. Skopa, "Downlink processing algorithms for multi-antenna wireless communications," *IEEE Communication Magazine*, 122–127, January 2005.

6. Astely, D., E. Dahlman, A. Furuskar, Y. Jading, M. Lindstrom, and S. Parkvall, "LTE: The evolution of mobile broadband," *IEEE Communication Magazine*, 44–51, April 2009.

7. Alamouti, S., "A simple transmit diversity technique for wireless communications," *IEEE J. Select Areas Communication*, Vol. 16, 1451–1458, October 1999.

8. Banister, B. C. and J. R. Zeidler, "A simple Gradient sign algorithm for transmit antenna weight adaptation with feedback," *IEEE Transactions on Signal Processing*, Vol. 51, No.5, 1156–1171, May 2003.

9. Litva, J. and T. K. Lo, *Digital Beamforming in Wireless Communications*, Artech house Inc., Norwood, MA, 1996.

10. Van Trees, H. L., *Optimum Array Processing*, John Wiley & Sons, Inc., New York, 2002.

11. Gerlach, D. and A. Paulraj, "Adaptive transmitting antenna arrays with feedback," *IEEE Signal Processing Letters*, Vol. 1, No. 10, 150–152, October 1994.

12. Godara, L. C., "Applications of antenna arrays to mobile communications, Part II: Beam-forming and direction of arrival considerations," *Proc. IEEE*, Vol. 85, No. 85, 1195–1245, August 1997.

13. Godara, L. C., "Applications of antenna arrays to mobile communications, Part II: Beam-forming and direction of arrival considerations," *Proc. IEEE*, Vol. 85, No. 85, 1195–1245, August 1997.

14. Rashid-Farrokhi, F., K. J. R. Liu, and L. Tassiulas, "Transmit beamforming and power control systems for cellular wireless systems," *IEEE J. Select. Areas Communications*, Vol. 16, No.

8, 1437–1450, October 1998.

15. Banister, B. C. and J. R. Zeidler, "Feedback assisted stochastic gradient adaptation of multi-antenna transmission," *IEEE Transactions on Wireless Communications*, Vol. 4, No.3, 1121–1135, May 2005.

16. Heath, Jr., R. W. and A. Paulraj, "A simple scheme for transmit diversity using partial channel feedback," *Conf. Rec. 32nd Asilomar Conference on Signals, Systems and Computers*, Nov. 1998.

17. Hottenin, A., O. Trikkonen, and R. Wichman, *Multi-antenna Transceiver Techniques for 3G and Beyond*, Wiley, New York, 2003.

18. Li, Q., G. Li, W. Lee, M. Lee, D. Mazzarese, B. Clerckx, and Z. Li, "MIMO techniques in WIMAX and LTE: A feature overview," *IEEE Communication Magazine*, 86–92, May 2010.

19. Hussain, S. S. I. and M. I. Shiekh, "A downlink tracking algorithm by adapting the beamspace weights of the transmit antenna," *IEEE International Conference on Electrical Engineering*, 1–6, April 2007.

20. Molisch, A. F., H. Asplund, R. Heddergott, M. Steinbauer, and T. Zwick, "The COST259 directional channel model-part I:overview and methodology," *IEEE Transactions On Wireless Communications*, Vol. 5, No. 12, 3421–3433, December 2006.

21. Eyceoz, T., A. Duel-Hallen, and H. Hallen, "Deterministic channel modeling and long range prediction of fast fading mobile radio channels," *IEEE Communications Letters*, Vol. 2, No. 9, 254–256, September 1998.

22. Shiu, D., G. J. Foschini, M. J. Gans, and J. M. Kahn, "Fading correlation and its effect on the capacity of multielement antenna systems," *IEEE Transactions on Communications*, Vol. 48, No. 3, 502–513, March 2000.

23. Sklar, B., *Digital Communications: Fundamentals and Applications*, Prentice Hall, Upper saddle River, New Jersey, December 2006.

24. Haykin, S., *Adaptive Filter Theory*, Pearson Education Pte. Ltd., Singapore, 2002.